Structure and Electronic Characteristics of Coronoid Polycyclic Aromatic Hydrocarbons as Potential Models of Graphite Layers with Hole Defects

Jerry Ray Dias*

Department of Chemistry, University of Missouri, Kansas City, Missouri 64110-2499

Received: August 5, 2008; Revised Manuscript Received: September 22, 2008

While the literature on coronoid hydrocarbons is comprehensively surveyed, new enumeration results on select coronoid classes are presented. The first examples of Kekuléan polycyclic (even-carbon) alternant hydrocarbons with doubly degenerate zero eigenvalues at the HMO level are identified. The parallelism between a molecule removed and the antimolecule hole left in formation of a graphite vacancy defect is elaborated. It is argued that the formation of a single carbon atom vacancy hole defect in graphite should be facile because it would entail a minimum electronic reorganization. These results are supported by a substantial amount of eigenvalue calculations. This work provides a unique overview for the class of coronoid hydrocarbons.

Introduction

Graphenes are well-defined, nanosized polycyclic aromatic hydrocarbons having potential uses in the fabrication of organic electronic devises.[1] Removal of a single carbon atom from a graphite system generates a point defect that is a one-atom hole (called a Schottky defect).[2] Extended graphite layers,[3] single-wall nanocones,[4] and soot platelets[5] may possess vacancy hole defects involving larger (multiatoms) holes which can be modeled by coronoids (circulenes),[6] which we will consider in this paper. The extensive work published on coronoids by Cyvin and co-workers can serve the reader with background.[7]

Results and Discussion

Nomenclature and Terminology. ***Terminology.*** A polyhex is the discrete mathematical equivalent of a benzenoid hydrocarbon. A polyhex is a tessellation (mosaic) of hexagons which corresponds to the molecular graph of a benzenoid. A molecular graph of a benzenoid hydrocarbon (used interchangeably with the term "benzenoid") is its σ-bond skeleton with all the carbons, hydrogens, and C−H and π-bonds not explicitly shown. The benzenoid formula notation (C_nH_s) for the total number of carbons (N_c), hydrogens (N_H), and σ-bonds is equivalent to the polyhex (molecular graph) graph-theoretical notation for total number of vertices (n), degree-2 vertices (s), and lines or edges (q), respectively. There are three distinct kinds of benzenoid carbons, the numbers of which are denoted by N_{pc}, N_{Ic}, and N_H ($N_c = N_{Ic} + N_{pc} + N_H$), where N_{pc} and N_{Ic} correspond to the peripheral and internal degree-3 molecular graph vertices and N_H corresponds to the degree-2 vertices. The subscripts i or I and p denote internal and peripheral, respectively. The number of hexagonal rings is denoted by r. A benzenoid is strained if it has two or more adjacent bay regions. Thus, benzo[c]phenanthrene is strained, but chrysene and triphenylene are essentially strain-free. Recall that strained benzenoids cannot be circumscribed and that leapfrog benzenoids are strain-free total resonant sextet (TRS) benzenoids.[8] The general terminology associated with benzenoids is directly applicable to coronoids.

In the application of the Euler relationship ($r + g = q - n + 1$), Hall introduced the genus (g) in reference to the number of hydrogen-containing corona holes; $g = 0$ for benzenoid hydrocarbons.[6] As will be seen, kekulene ($C_{48}H_{24}$), a single-coronoid hydrocarbon, has a genus of $g = 1$. In general, a multiple coronoid of genus g will be a g-tuple coronoid (single, $g = 1$; double, $g = 2$; triple, $g = 3$; etc.) in our terminology.

Cycloarenes. In their paper reporting the first synthesis of kekulene (Figure 1), Staab and Diederich[9] defined cycloarenes as being polycyclic aromatic compounds made by a combination of angular and linear fused benzene units enclosing a cavity into which carbon−hydrogen bonds point, with all members having molecular masses that are multiples of 50 (corresponding to C_4H_2). The minimum number of hydrogens in such a cavity is 2, and all cycloarenes by necessity must be Kekuléan and closed catacondensed systems which may be either alternant or nonalternant hydrocarbons. As such cycloarenes belong to a subclass of circulenes or coronoids. Staab and Diederich also suggested a possible unambiguous nomenclature for their cycloarenes: Proceeding clockwise through the macrocycle, each annellation is related to the previous one by labeling as "*a*" the bond of fusion between two benzene rings and then alphabetically marking the subsequent bonds of the individual rings in a clockwise fashion, which then leads to "*d*" for linear and "*e*" for angular annellations. In this way kekulene is formally named cyclo[*d.e.d.e.d.e.d.e.d.e.d.e*]dodecakisbenzene. Staab and co-workers have also reported the first synthesis of cyclo[*d.e.d.e.e.d.e.d.e.e*]decakisbenzene (cf. with $C_{40}H_{20}$ in Figure 1, which has also been called "clarene").[10]

Figure 2 gives the molecular graphs of the first-generation (shown in bold) and second-generation members belonging to the benzenoid constant one-isomer series resulting from our successive circumscribing algorithm ($C_nH_s \rightarrow C_{n+2s+6}H_{s+6}$);[11] these benzenoids have been shown to be important intermediates in flames by time-of-flight mass spectrometric sampling of flames.[12] Removal of the ultimate excised internal structures from these second-generation 1-isomers (i.e., central edge, carbon vertex (methyltriyl), ethenetetrayl, allylpentayl, benzenehexayl, benzylheptayl) gives the respective cycloarenes shown in Figure 1. The $C_{40}H_{20}$ and $C_{48}H_{24}$ (kekulene) cycloarenes have been synthesized by Funhoff and Staab and Staab and Diederich, respectively.[9,10] The IUPAC name for the $C_{40}H_{20}$ cycloarene is 13,17:14,18-dimethenoanthra[1,2-*a*]benzo[*o*]pen-

* E-mail: diasj@umkc.edu.

10.1021/jp806987f CCC: $40.75
Published on Web 11/05/2008

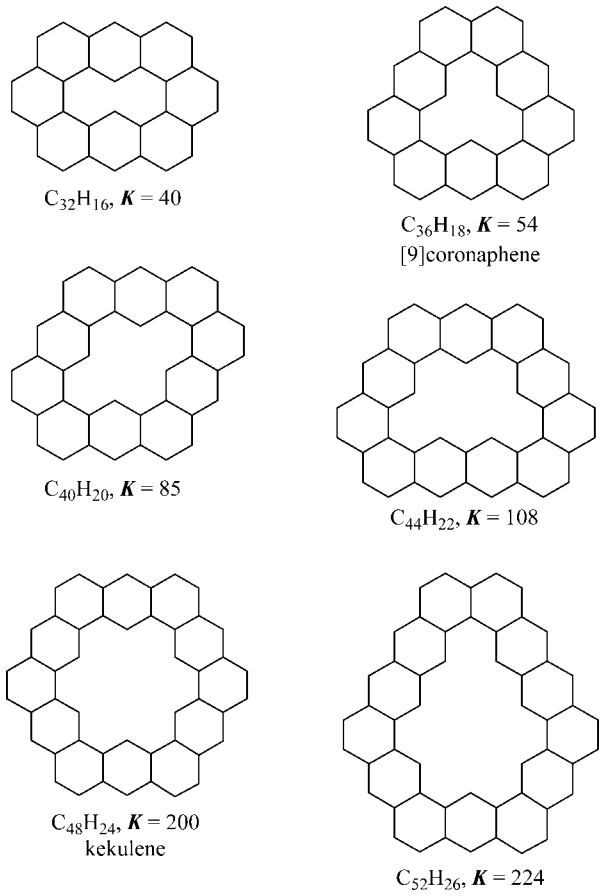

Figure 1. Cycloarenes (primitive coronoids) formed from the second-generation members of the 1-isomer series by excising out their ultimate excised internal structures.

taphene. In Figure 2, it should be noted that the molecular graphs of the Kekuléan (even-carbon) benzenoids ($C_{32}H_{14}$, $C_{42}H_{16}$, $C_{54}H_{18}$) have an even number of internal degree-3 vertices and the removal of an even number of internal degree-3 vertices generates Kekuléan cycloarenes ($C_{32}H_{16}$, $C_{40}H_{20}$, $C_{48}H_{24}$) and the molecular graphs of the monoradical (odd-carbon) benzenoids ($C_{37}H_{15}$, $C_{47}H_{17}$, $C_{59}H_{19}$) have an odd number of internal degree-3 vertices and the removal of an odd number of internal degree-3 vertices also generates Kekuléan cycloarenes ($C_{36}H_{18}$, $C_{44}H_{22}$, $C_{52}H_{26}$). In the former cycloarene set, the inner and outer rims are comprised of aromatic (pπ-bonds with $4n + 2$ electrons) annulene circuits, and in the latter cycloarene set, the inner and outer rims are comprised of antiaromatic (pπ-bonds with $4n$ electrons) annulene circuits. No representative of the latter set of cycloarenes with antiaromatic circuits has yet been synthesized, though Staab and co-workers[13] have reported their synthesis of precursors and failed attempts to convert them to the $C_{36}H_{18}$ cycloarene ([9]coronaphene).

The resonance energies per electron (REPE) for the primitive coronoids in Figure 1 are presented in Table 1. In general, the coronoids having antiaromatic outer and inner perimeters have lower REPE compared to those that do not. The conjugated circuit-derived resonance energies of all the Figure 1 coronoids except the last one have been published in Table 24 of a paper by Randić.[14]

Coronoids and Circulenes. To emphasize that in this paper we restrict ourselves mainly to polyhex systems that can be cut out of a perfect graphite layer, the term coronoid will be used. According to Cyvin and co-workers, a single coronoid (one-hole benzenoid-related systems) is obtained from a benzenoid

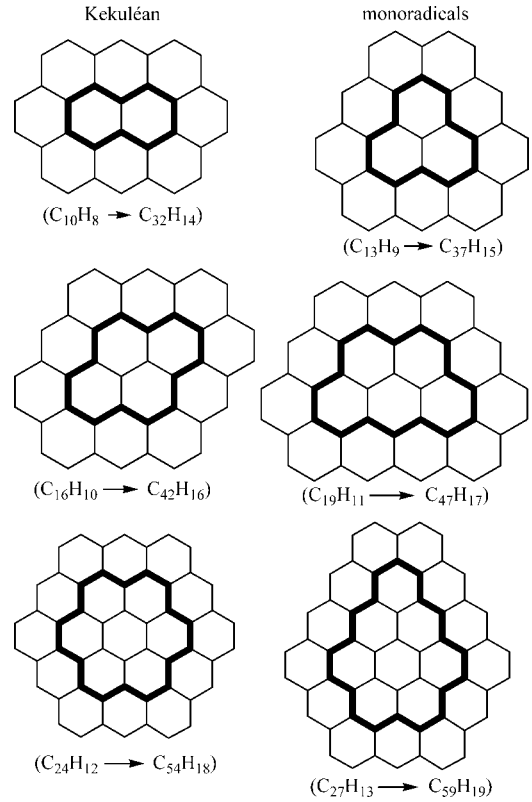

Figure 2. First-generation (in bold) and second-generation members of the 1-isomer series identified in flames.

TABLE 1: Electronic Parameters of the Primitive Coronoid Hydrocarbons in Figure 1

coronoid	K	REPE[a]	REPE[b]	REPE[c]	E_π (β)	E_{HOMO} (β)
C32H16	40	0.131	0.137	0.105	45.8578	0.4016
C36H18	54	0.124	0.131	0.099	51.4703	0.3042
C40H20	85	0.128	0.132	0.101	57.2087	0.3801
C44H22	108	0.125	0.126	0.096	62.8189	0.2781
C48H24	200	0.127	0.131	0.101	68.6102	0.4372
C52H26	224		0.123	0.094	74.1700	0.2732

[a] Randić, conjugated circuit in electronvolts per pπ electron. [b] Herndon, 1.185 ln K in electronvolts per pπ electron. [c] Hess and Schaad, in electronvolts per pπ electron ($\beta = 2.23$ eV/electron).

by deleting some internal vertices and/or edge(s) so that a hole with the size of at least two hexagons emerges and is completely surrounded by hexagons.[7] Allowance is made for more than one hole ($g = 1$) by introducing the terms double coronoid ($g = 2$) for two holes, triple coronoid ($g = 3$) for three holes, etc. They are all alternant hydrocarbons (AHs). Like a benzenoid, a coronoid is said to be pericondensed if it has at least one internal carbon vertex ($N_{Ic} > 0$); otherwise it is catacondensed. A pericondensed coronoid is strictly pericondensed if it has no catacondensed appendages or segments and has a connected excised internal structure. Single coronoids with one hole ($g = 1$) surrounded by a single shell of hexagons are called primitive coronoids. Primitive coronoids belong to a subclass of the catacondensed coronoids which may have catacondensed appendages.[15] Monocirculenes follow this definition except the hole can include other polygon sizes. Class I circulenes are coronoids (without the preceding terms of mono or single) which can include multiholes each with at least two hexagons. Class I circulenes or coronoids require holes into which carbon−hydrogen bonds point.

Class II circulenes have holes other than hexagonal or benzenoid-shaped and may be nonalternant hydrocarbons (non-

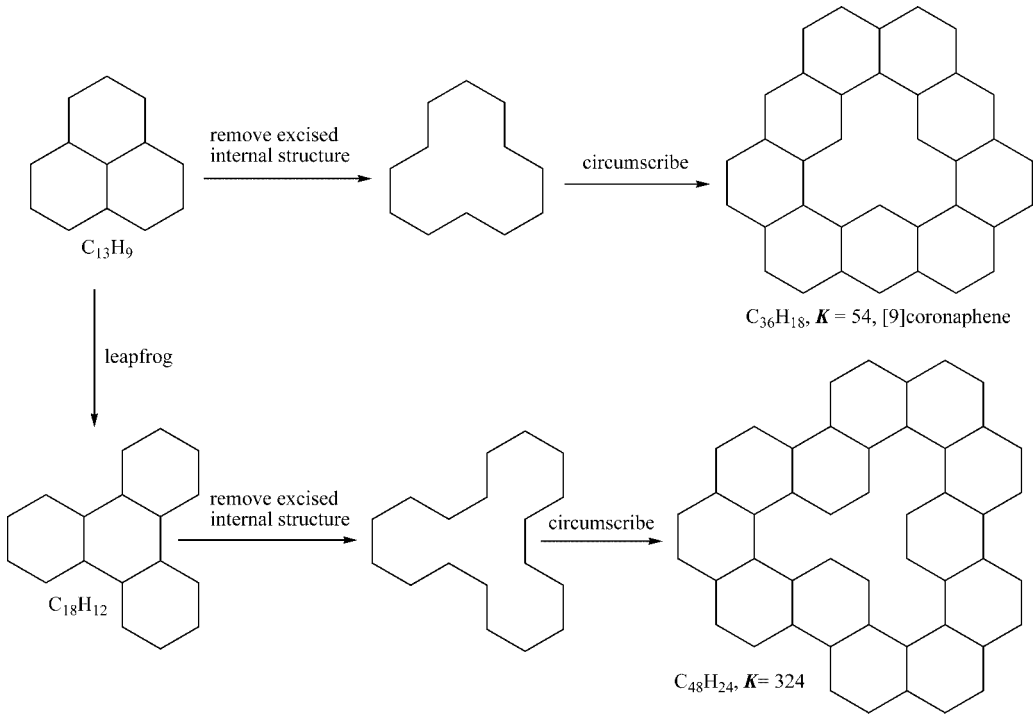

Figure 3. Illustration of the algorithm for generation of the only $C_{36}H_{18}$ and $C_{48}H_{24}$ primitive coronoid hydrocarbons.

AHs). [5]Circulene corresponds to corannulene ($C_{20}H_{10}$), which is a well-known bowl-shaped molecule with a pentagonal hole.[16] Successive circumscribing of corannulene leads to the C_{5h} fluoranthenoid/fluorenoid 1-isomer series.[17] Large members of this 1-isomer series represent one of the simplest classes of nanocones.[4,18] [7]Circulene ($C_{28}H_{14}$, a non-AH with a heptagonal hole) has also been synthesized and studied and is a saddle-shaped molecule.[19] Also, [7,7]circulene ($C_{40}H_{18}$) having a heptalene-like bihole has been synthesized;[20] if it was not for the central bridging bond in [7,7]circulene, one would have a single hole shaped like heptalene and the molecule would carry the name of 2H-[12]circulene, where the 2H prefix indicates two inward-pointing hydrogens. The MMPM1 strain energies for several coronoids and a $C_{40}H_{20}$ circulene with a hole shaped like corannulene has been reported by Lahti.[21] A precursor to this $C_{40}H_{20}$ circulene (a non-AH cycloarene) and the failed attempt to convert it to the $C_{40}H_{20}$ circulene has been reported.[13]

Topological Properties of Coronoids. The number of peripheral degree-3 vertices, N_{pc}, on the outer perimeter of a benzenoid (polyhex) molecular graph is $N_{pc} = N_H - 6$. There can be 0, 1, 2, 3, and 4 successive degree-2 vertices between any two nearest peripheral degree-3 vertices designated as bay, solo, duo, trio, and quarto regions, respectively. η_0, η_1, η_2, η_3, and η_4 designate the number of bay, solo, duo, trio, and quarto peripheral regions on a given benzenoid molecular graph. For catacondensed systems $\eta_3 = 0$ and strictly pericondensed systems $\eta_4 = 0$. The outer perimeter topology of any benzenoid molecular graph is described by $-\eta_0 + \eta_2 + 2\eta_3 + 3\eta_4 = 6$, which is independent of the number of solo regions (η_1); also $N_H = \eta_1 + 2\eta_2 + 3\eta_3 + 4\eta_4$.[22] In analogy, the topology for the coronoid hole is described by $N_{pc}' = N_H' + 6$ and $-\eta_0' + \eta_2' + 2\eta_3' + 3\eta_4' = -6$, where the prime emphasizes that these relationships are for the inner perimeter associated with the corona hole. Note the change in sign before the number 6 in going to the latter equations.[3]

Some New Enumeration Results for Select Coronoid Hydrocarbon Subclasses. ***Primitive Coronoids.*** Primitive coronoid (pc) hydrocarbons have a single ($g = 1$), hydrogen-containing, benzenoid-shaped hole surrounded by a single shell of hexagons and are a subclass of the catacondensed coronoids (i.e., $N_{Ic}(pc) = 0$ and $\eta_4 = 0$).[23] Their formulas have $N_c = 2N_H$. All the cycloarenes in Figure 1 are primitive coronoids. We remind the reader that herein we restrict ourselves to polyhex systems that can be cut out of a perfect graphite layer. Primitive coronoids are always even-carbon, unbranched catacondensed systems ($N_{Ic} = 0$), where their number of hexagonal rings is $r(pc) = (1/2)N_H(pc)$. The algorithm for their generation is as follows: (a) Identify all the structures of (ordinary) benzenoids having the same number of hydrogens (N_H) to serve as templates (core structures) for the hole (cf. with the diagonal arrays of formulas in Table PAH6);[3,11] note that N_H of the core benzenoid structures will equal the number of rings (r(pc)) of the successor primitive coronoid. (b) Delete all those benzenoids having coves (two adjacent bay regions), fjords (three adjacent bay regions), or more adjacent bay regions. (c) The remaining benzenoids will serve as holes by removing their excised internal structure, which may be only internal edges, leaving their perimeters, which are circumscribed without changing their shape. Figure 3 illustrates this process. This generates all primitive coronoids having the number of rings corresponding to the initial number of hydrogens of the template benzenoids; i.e., the number of hydrogens in the initial benzenoid template doubles in the successor primitive coronoid. To illustrate this, consider the molecular graph of phenalenyl ($C_{13}H_9$) shown in Figure 3. This is the only possible benzenoid having nine hydrogens, and excising out the only internal degree-3 vertex from its center gives the C12 circuit, which when circumscribed without changing its shape gives the only molecular graph corresponding to the $C_{36}H_{18}$ coronoid hydrocarbon ([9]coronaphene). The general formula of primitive coronoids ($C_{28+4n}H_{14+2n}$, $n = 1, 2, 3, 4,...$) is a formula belonging to the $N_{Ic} = 6$ row series of Table PAH6 (i.e., $N_c = 2N_H$),[3,17] thus accounting for the molecular mass magic number of 50 noted by Staab and Diederich.[9] In this way (Figure 3) from all the known benzenoid structures of a given number of hydrogens, one can enumerate all the primitive coronoid structures of a given number of rings.

From the depictions in the book of Knop and co-workers[24] and this algorithm, we were able to enumerate the following numbers of primitive coronoids for r(pc) = 8−14, in agreement with the work of Brunvoll and co-workers:[23] $C_{32}H_{16}$ (1), $C_{36}H_{18}$ (1), $C_{40}H_{20}$ (3), $C_{44}H_{22}$ (2), $C_{48}H_{24}$ (11), $C_{52}H_{26}$ (12), $C_{56}H_{28}$ (40).

Hollow Coronoids. Hollow coronoids belong to a subclass of the primitive coronoids which in turn is a subclass of catacondensed coronoids. A hexagon of a primitive coronoid is either linearly or angularly annelated. The angularly annelated hexagons of a primitive coronoid are called corners. They may be protruding on the coronoid outer perimeter or intruding within its inner perimeter associated with the hole. A hollow coronoid is a primitive coronoid with no intruding corners. There are only 16 hollow coronoids out of 70 primitive coronoids and 90 932 total coronoids with $r < 15$.[25] A protruding or intruding corner corresponds to a duo region. The number of protruding and intruding corners corresponds to η_2 and η_2', respectively. Thus

$$\eta_2 = \eta_2' + 6 \tag{1}$$

A segment of a primitive coronoid is defined as a linear succession of hexagons between two corners inclusive. Each corner belongs to two neighboring segments. The number of segments (S) is equal to the number of corners, namely

$$S = \eta_2 + \eta_2' \tag{2}$$

Inserting (1) into (2) gives

$$S = 2\eta_2' + 6 \tag{3}$$

A hollow coronoid is a primitive coronoid with exactly six protruding corners and no intruding corners ($\eta_2 = 6$ and $\eta_2' = 0$) and consequently six segments, i.e., $S = 6$. All the primitive coronoids in Figure 1 are also hollow coronoids. Hollow coronoids (hpc) have special topological properties which can be exploited. The following properties can be verified from the hollow coronoids in Figure 1: $\eta_2 = \eta_0'$, $\eta_1 = \eta_1'$, and $\eta_3' = \eta_3 = \eta_4' = \eta_4 = 0$. The inner dual of hollow coronoids are a six-sided polygon in which opposing sides are all parallel. The inner dual is constructed by placing a point within each hexagon and connecting each pair of adjacent points within two hexagons sharing an edge with a line.

This subclass can be enumerated as by the algorithm above, but in step b the core benzenoid structures selected as templates must also be devoid of bay regions ($\eta_0 = 0$). Thus, we were able to enumerate the following numbers of hollow primitive coronoids for r(hpc) = 8−15, in agreement with the work of Cyvin and co-workers:[25] $C_{32}H_{16}$ (1), $C_{36}H_{18}$ (1), $C_{40}H_{20}$ (2), $C_{44}H_{22}$ (1), $C_{48}H_{24}$ (4), $C_{52}H_{26}$ (2), $C_{56}H_{28}$ (5), $C_{60}H_{30}$ (4). The number of nonisomorphic hollow coronoids for a given number of rings up to r(hpc) = 50 (starting at r(hpc) = 8) has been published by Cyvin and co-workers.[25] Keeping in mind that r(pc) = ($^1/_2$)N_H(pc) and N_c(pc) = $2N_H$(pc), we now list those numbers in sequence ($C_{4r}H_{2r}$): 1, 1, 2, 1, 4, 2, 5, 4, 7, 5, 11, 7, 13, 11, 17, 13, 23, 17, 27, 23, 33, 27, 42, 33, 48, 42, 57, 48, 69, 57, 78, 69, 90, 78, 106, 90, 118, 106, 134, 118, 154, 134, 170. The repetitive pattern of a, b, c, a,... should now be obvious to the reader. On the basis of this pattern, we can extrapolate the number of hollow coronoids for the formulas r(hpc) = 51 and r(hpc) = 53: $C_{204}H_{102}$ (154) and $C_{212}H_{106}$ (170). This repetitive pattern and the extrapolated results were not recognized by Cyvin and co-workers and are presented herein for the first time.

Fibonacenic Coronoids. Fibonacenic coronoid (fpc) hydrocarbons belong to a special subclass of primitive coronoids that have no linear sequence of three or more benzenoid rings as in anthracene or higher acenes.[26] These systems always have an even number of rings. Fibonacenic coronoids having r rings have their number of Kekulé structures given by $K = F_{r+1} + F_{r-1} + 2$, where F_i is the ith Fibonacci number. In general $N_c = 4r$ for all primitive systems. A unique property of these systems is that each benzenoid ring has an equal share in the Kekulé structure count. This results in all rings having the same partition of electrons ($P_j = 4$). For each Kekulé structure, electrons are partitioned in each individual benzenoid ring by assigning two electrons of a double bond not being shared by another ring and one electron of a double bond shared by two rings; summing all the ring electron counts for all Kekulé structures and dividing the result by the number of Kekulé structures gives the electron content (P_j) for each ring j.

Balaban and Randić[26] also discussed twisted-ring-like coronoids shaped like an "8". While these systems might be good models for some types of screw dislocation defects in graphite, such systems are excluded in this paper.

The planar fpc subclass can be enumerated as by the algorithm above, but the core template benzenoid selected must be a member of the essentially strain-free TRS benzenoids.[8,27] Thus, starting with triphenylene ($C_{18}H_{12}$), the smallest and only TRS of 12 hydrogens, and deleting the three internal edges gives the C18 circuit, which when circumscribed without changing its shape gives the molecular graph corresponding to the only $C_{48}H_{24}$ fibonacenic coronoid as shown in Figure 3. Using our data in Table 2 of ref 27, we were able to enumerate the following isomer numbers for fibonacenic primitive coronoids ($C_{4r}H_{2r}$) for r(fpc) = 12, 14, 16, 18, 20, 22, 24, 26, 28: $C_{48}H_{24}$ (1), $C_{56}H_{28}$ (1), $C_{64}H_{32}$ (1), $C_{72}H_{36}$ (4), $C_{80}H_{40}$ (5), $C_{88}H_{44}$ (15), $C_{96}H_{48}$ (29), $C_{104}H_{52}$ (81), $C_{112}H_{56}$ (>133). The sole isomers of $C_{48}H_{24}$ and $C_{56}H_{28}$ were first depicted by Brunvoll and co-workers,[23] and the isomers of $C_{64}H_{32}$ and $C_{72}H_{36}$ were first depicted by Balaban and Randić.[26] Every ring of all fibonacenic primitive coronoid hydrocarbons has an electron content of 4 ($P_j = 4$) and is derived from TRS benzenoid hydrocarbons. Fibonacenic coronoids have the highest Kekulé structure count (K) of all primitive coronoids, and TRS benzenoids have the highest K of all benzenoids; both these subclasses have unique properties which suggest that there must be some fundamental principle operating here. With few exceptions for any given primitive coronoid isomer set, the hollow coronoids have among the lowest number of outer perimeter bay regions (i.e., $\eta_0 = 0$) and K values. The fibonacenic coronoids for any given primitive coronoid isomer set have the highest K values.

Total Resonant Sextet Polycyclic Aromatic Systems. The first examples of TRS coronoid hydrocarbons were probably depicted in a paper by Cyvin and co-workers.[28] They do not belong to the primitive subclass and are not leapfrog TRS coronoids. Given the success of Müllen and co-workers in synthesizing large TRS benzenoids,[29] we believe the members of the TRS coronoid class offer the most likely targets for future experimental synthesis.

Figure 4 shows the smallest coronoid hydrocarbon ($C_{32}H_{16}$, ovalene with a naphthalene-shaped hole) and its circumscribed successor ($C_{66}H_{22}$); this latter is the smallest strictly pericondensed coronoid. Recall strictly pericondensed means those polycyclic aromatic systems having no catacondensed appendages (branches) or segments or disconnected excised internal structures. The formulas for all such circumscribed primitive coronoids appear in the $d_s = -7$ column series of Table PAH6,[11] and $N_c = 3N_H$. Performing the leapfrog algorithm on this smallest $C_{66}H_{22}$ strictly pericondensed coronoid gives the smallest leapfrog TRS coronoid ($C_{132}H_{44}$), which has a circo-

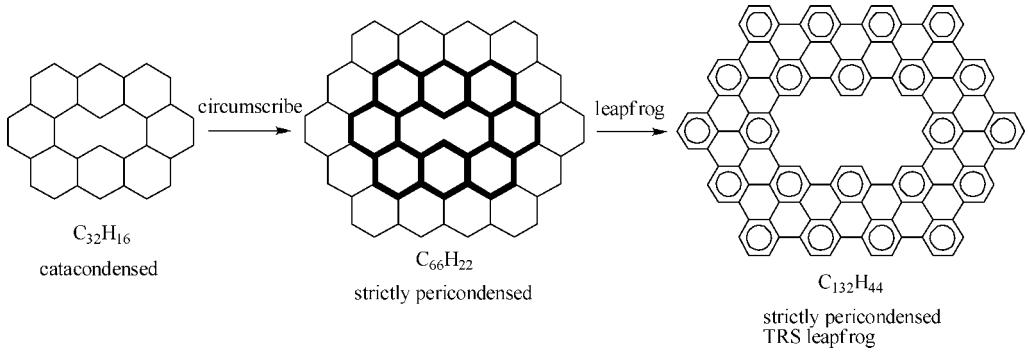

Figure 4. Circumscribing the smallest catacondensed coronoid gives the smallest strictly pericondensed coronoid, which upon leapfrogging gives the smallest leapfrog TRS coronoid.

biphenyl-shaped hole. Recall that the leapfrog of naphthalene gives biphenyl, and circumscribing biphenyl gives circobiphenyl (using Clar's nomenclature).

Point defects can be modeled by missing atoms in an otherwise large polycyclic aromatic hydrocarbon (graphene). A single missing atom in hexabenzo[*a*,*f*,*k*,*p*,*u*,*z*]circumcoronene ($C_{78}H_{30}$) from one of six equivalent central inner sites (Schottky defect) gives a monoradical ($C_{77}H_{33}$) which was discussed by Dietz and co-workers;[2] the precursor, hexabenzo[*a*,*f*,*k*,*p*,*u*,*z*]circumcoronene, is a TRS benzenoid that was featured as an HMO problem (p 109) by Dias[30] and subsequently synthesized by Müllen and co-workers.[31] Simultaneously removing all six equivalent central inner sites (i.e., benzenehexayl or hexadehydrobenzene) and installing six hydrogens within the cavity thus formed gives the $C_{72}H_{36}$ TRS coronoid depicted by Cyvin and co-workers.[28] TRS polycyclic aromatic systems have the largest *K* values when compared on an isomer basis. A number of papers dealing with enumeration of *K* for coronoids and Möbius coronoids have been published.[32]

Kekulene (Cyclododecakisbenzene). Kekulene ($C_{48}H_{24}$), synthesized by Staab and Diederich,[9] represents the prototype for a benzenoid graphene with a multiatom deficit hole. In a formal sense, the kekulene structure can be generated from circumcoronene ($C_{54}H_{18}$) by excising out the benzene carbon core and attaching six hydrogen atoms to the dangling bonds created within the hole (cavity). A hexaazakekulene ($C_{42}H_{18}N_6$) D_{6h} isomer with six cavity nitrogens that needs no inner hydrogen atom supplements was the ultimate synthetic goal of a study by Ransohoff and Staab, which has not yet been accomplished.[33] However, it should be noted that a D_{3h} hexaazakekulene isomer with three outer and three inner nitrogens has been synthesized.[34] The synthesis of kekulene was motivated by the ideas that it might be superaromatic and that ring currents would affect the ^{1}H NMR chemical shift of the inner cavity hydrogens differently from that of the outer hydrogens. Because of its planar cyclic conjugation and D_{6h} symmetry, kekulene became regarded as "superbenzene", and there was interest in evaluating to what extent the diatropicity in the macrocyclic 18- and 30-annulene $4n + 2$ circuits would compete with the ring current induction within the benzene subunits. In regard to the latter, the inner cavity hydrogens of kekulene exhibited a chemical shift of 10.47 ppm, and in hexaazakekulene, the inner cavity hydrogens gave a chemical shift of 12.98 ppm, where the influence of two cavity nitrogens acting on each cavity hydrogen causes a deshielding of 2.5 ppm. These results conform to our own work, which showed that the influence of a single nitrogen nonbonding electron pair located within a similar bay region resulted in a deshielding effect of 0.9 ppm; 2 times 0.9 ppm should be compared with 2.5 ppm.[35]

The reported experimental ^{1}H NMR chemical shifts for the $C_{40}H_{20}$ and $C_{48}H_{24}$ cycloarene outer protons range from 8.0 to 8.2 ppm (duo) and from 8.45 to 8.65 ppm (solo) and for the inner protons from 9.5 to 10.5 ppm (solo embedded between bay regions). These chemical shifts are reproduced by the calculated values of Vogler.[36]

Superaromaticity. The name kekulene and the term superbenzene were coined by Staab in 1965 at the Kekulé Centennial Meeting in Bonn. Thus, the superaromatic concept emerged from this meeting, which has inspired several adaptations besides kekulene. In regard to his sextet polynomial, Hosoya introduced the definition of supersextet as occurring in the middle ring of the coronene substructure.[37]

The superaromaticity of kekulene has been discounted along different lines of reasoning. Superaromaticity is defined as extra stabilization due to macrocyclic conjugation in super-ring molecules, such as kekulene; it represents a small part of global aromaticity, which is measured by TRE. According to the conjugated circuit theory of Randić, the contribution of $4n + 2$ circuits rapidly decreases with increasing size, and circuits larger than 18 π-centers make little to no contribution to the resonance energy (RE) for aromatic systems. In fact, the REPE of kekulene is not extraordinary and is even smaller than that of other coronoids (Table 1). On the basis of the lack of significant extra stabilization energy, extra magnetic susceptibility exaltation, and anisotropy, and the NICS values, Jiao and von Rague Schleyer concluded that kekulene is not superaromatic.[38] Previously Aihara reached the same conclusion and recently presented a simple method for evaluating superaromaticity.[39]

Coronoids as Models for Vacancy Hole Defects in a Perfect Graphite Layer. ***Elementary Hole Defects.*** Now let us take the molecular graph of an even-carbon Kekuléan benzenoid (graphene) and excise out a carbon vertex. Since the resulting coronoid is an odd-carbon species, it must also be a radical system. Figure 5 illustrates this with dicircumcoronene ($C_{54}H_{18}$). The resulting radical ($C_{53}H_{21}$) coronoid has a cavity comprised of an inner antiaromatic annulene circuit and an outer perimeter comprised of an aromatic annulene circuit. To minimize the antiaromatic contribution of the inner annulene, the radical electron spends more than 40% of the time at the inner rim. This is representative of the most elementary hole defect where there is a local imbalance of starred and unstarred sites. According to the resonance-theoretic picture of such a hole in the infinite graphite lattice, the radical electron should be confined 100% of the time at the inner rim.

Now let us take the molecular graph of an even-carbon Kekuléan benzenoid and excise out different arrangements of even-carbon vertices, where the structure of one corresponds to a Kekuléan conjugated carbon system and that of another to

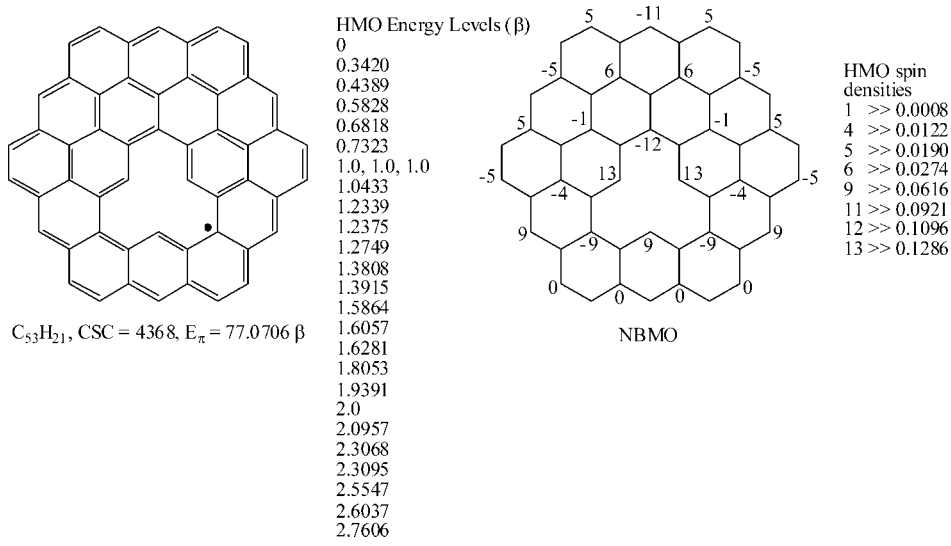

Figure 5. The radical hole in circumcoronene is comprised of an inner antiaromatic annulene circuit and an outer aromatic annulene ring. The unnormalized eigenvector for the nonbonding molecular orbital (NBMO) is given on the right structure. To minimize the antiaromatic contribution of the inner annulene, the radical electron spends more than 40% of the time at the inner rim.

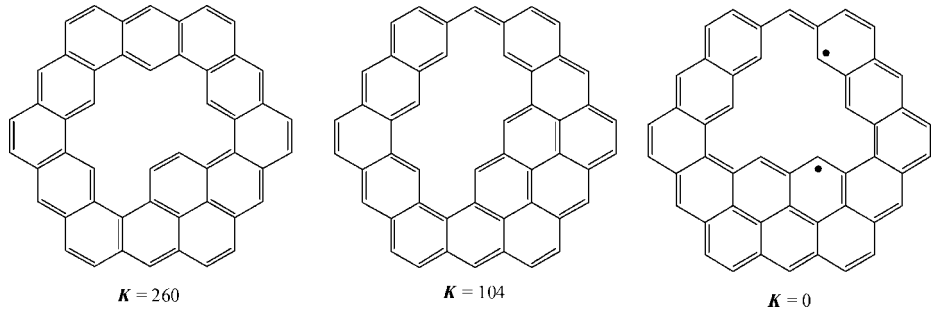

Figure 6. Removal of the C4 carbon skeletons of *s-cis*-1,3-butadiene, *s-trans*-1,3,butadiene, and trimethylenemethane diradical (C_4H_6) from circumcoronene ($C_{54}H_{18}$) generates the two Kekuléan and one diradical $C_{50}H_{24}$ circulenes after installation of six cavity hydrogens, repectively, as shown above.

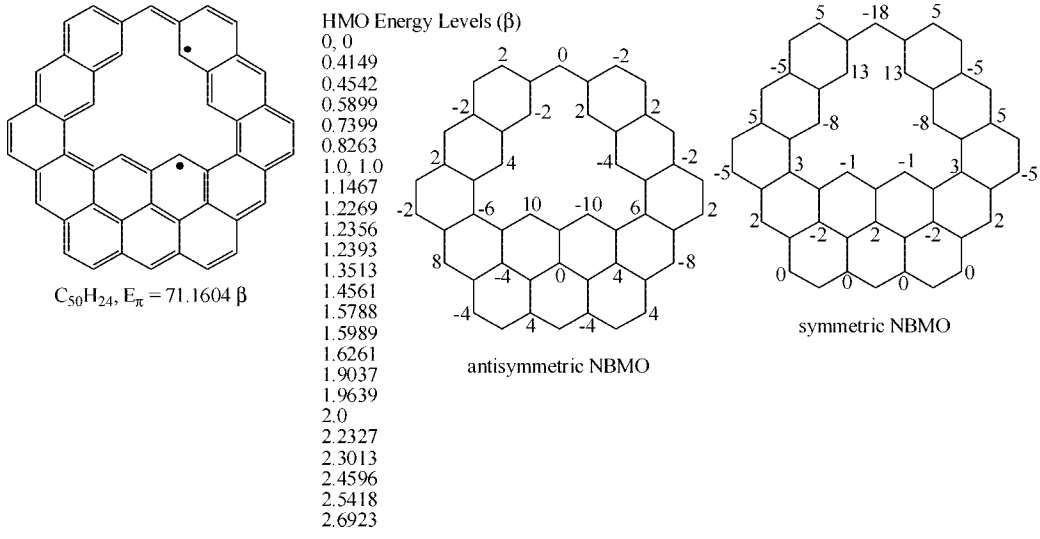

Figure 7. HMO data on the diradical hole.

its nondisjoint diradical isomer. Figure 6 illustrates the results using the D_{6h} $C_{54}H_{18}$ benzenoid hydrocarbon precursor for the carbon skeletons of the smallest nondisjoint diradical, trimethylenemethane diradical, and its Kekuléan isomers, *s-cis*- and *s-trans*-1,3-butadiene. Excising out a Kekuléan carbon cluster, such as *s-cis*- or *s-trans*-1,3-butadiene, will generate a Kekuléan coronoid, whereas excising any nondisjoint diradical carbon cluster, such as trimethylenemethane diradical, from a perfect hexagonal graphite layer or graphene molecule such as the D_{6h} $C_{54}H_{18}$ benzenoid will generate a diradical hole. Note that the inner perimeter of the hole and outer perimeter of these successor $C_{50}H_{24}$ coronoids are both comprised of aromatic annulene circuits. The first coronoid in Figure 6 is a benzokekulene with two degree-3 internal vertices and having $K = 260$. Kekulene in Figure 1 has 200 resonance structures ($K = 200$). This benzokekulene has a benzo[*ghi*]perylene-shaped hole

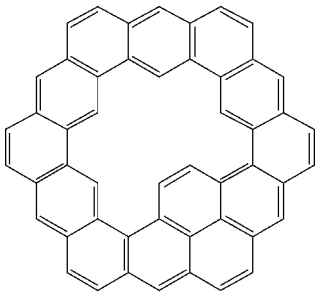

$C_{50}H_{24}$, $\boldsymbol{K}$ = 260, E_π = 71.7499 β

HMO Energy Levels (β)
0.3540
0.44115
0.4870
0.58855
0.5908
0.9576
1.0, 1.0, 1.0
1.2355
1.2360
1.3288
1.34355
1.5233
1.5450
1.5964
1.6017
1.8131
1.9287
2.0
2.2940
2.2966
2.5208
2.5443
2.6481

Figure 8. HMO data for benzokekulene.

(b[*ghi*]p-hole). In Figure 6, the second coronoid has an anthanthrene-shaped hole (A-hole), and the last one has a triangulene-shaped hole (T-hole). Using the thermochemical Benson group contributions[40] and assuming an infinite graphite lattice, we can calculate the relative enthalpy values (kcal/mol) for formation of these differently shaped holes:

$$\Delta H_f^\circ(\text{bp hole formation}) = \Delta H_f^\circ(\text{b[}ghi\text{]p-hole}) + \Delta H_f^\circ(1,3\text{-}C_4H_6) - \Delta H_f^\circ(\text{graphite}) - \Delta H_f^\circ(6H_2) = 64.2 + 26.1 - 31.9 - 0 = 58.4 \quad (4)$$

$$\Delta H_f^\circ(\text{A-hole formation}) = \Delta H_f^\circ(\text{A-hole}) + \Delta H_f^\circ(1,3\text{-}C_4H_6) - \Delta H_f^\circ(\text{graphite}) - \Delta H_f^\circ(6H_2) = 66.4 + 26.1 - 31.9 - 0 = 60.6 \quad (5)$$

$$\Delta H_f^\circ(\text{T-hole formation}) = \Delta H_f^\circ(\text{T-hole}) + \Delta H_f^\circ(C_4H_6) - \Delta H_f^\circ(\text{graphite}) - \Delta H_f^\circ(6H_2) = 71.9 + 47.7 - 31.9 - 0 = 87.7 \quad (6)$$

In the formation of the triangulene-shaped hole, our enthalpy calculation assumed that trimethylenemethane diradical converted to methylenecyclopropane (C_4H_6) as it was ejected. The results for the triangulene-shaped hole probably represent a lower bound since the Benson group contributions are less reliable for polycyclic alternant hydrocarbon (PAH) radical systems because of the lack of experimental data for radicals.[40] This enthalpy order matches the order of stability of the carbon molecule removed in the formation of the cavity hole defect in graphite.

With the exception of concealed benzenoid radicals, excising any radical benzenoid from a perfect hexagonal graphite layer will generate a radical circulene-like graphite system. In general, excising any nondisjoint diradical, such as trimethylenemethane diradical, from a perfect hexagonal graphite layer will generate a diradical hole. This observation of excising a nondisjoint even-carbon diradical from an even-carbon benzenoid to generate a diradical coronoid is a sort of complementary principle (removal of a carbon molecule generates a matching antimolecule hole) previously noted by Ivanciuc, Klein, and Bytautas.[41]

The important principle that emerges is that the characteristics of a graphite vacancy hole (antimolecule) can be deduced from our knowledge of the carbon molecules removed in their formation. Hall showed that making an anthracene hole versus a phenanthrene hole in circumperylene ($C_{50}H_{18}$) gave isomeric $C_{50}H_{22}$ coronoids where the former ($E_\pi = 72.1894\ \beta$ and $E_{HOMO} = 0.1064\ \beta$) was less stable than the latter ($E_\pi = 72.4384\ \beta$ and $E_{HOMO} = 0.2299\ \beta$); this parallels the relative stability of anthracene versus phenanthrene. This relative order also coincides with the conjugated circuit-derived resonance energies for two isomeric $C_{40}H_{20}$ primitive coronoids, one with an anthracene-shaped hole (REPE = 0.116 eV) and the other with a phenanthrene-shaped hole REPE = 0.150 eV).[42]

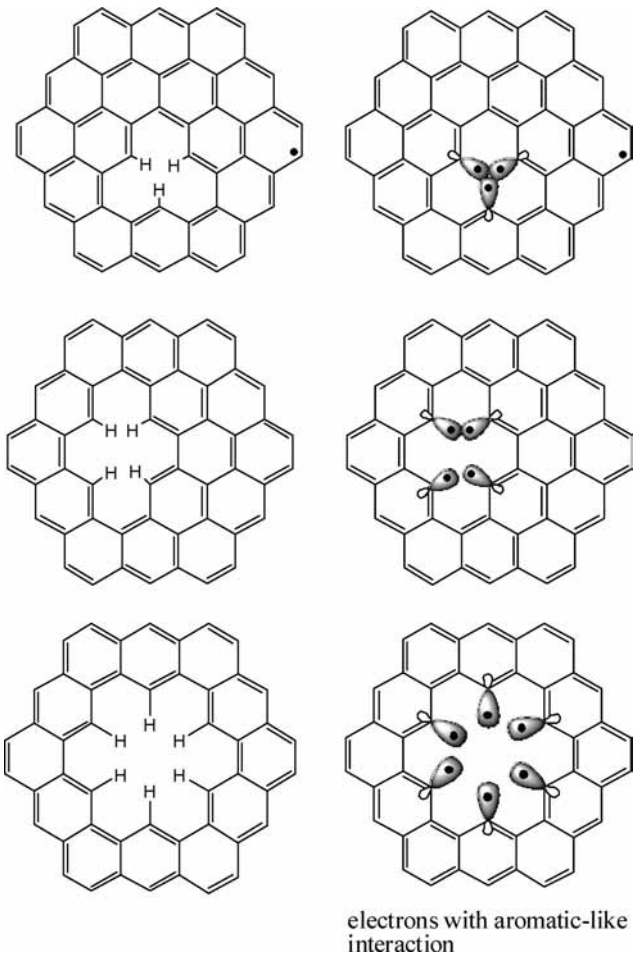

Figure 9. Bonded hydrogens versus interacting electrons belonging to dangling bonds within a coronoid cavity.

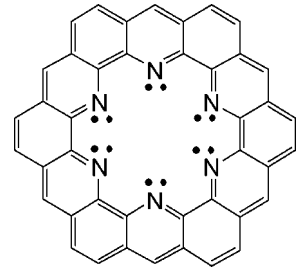

Figure 10. Hexaazakekulene would have 12 interacting electrons within its cavity, resulting in antiaromatic destabilization.

Dangling Hybrid Orbitals within the Vacancy Hole Defect. In the vacancy holes modeled in Figures 5−8, it was assumed that hydrogens were installed within the hole. In principle, dangling hybrid orbitals can occur within the hydrogen devoid vacancy hole defect as shown in Figure 9. Dangling hybrid orbitals have been extensively discussed in the theory of silicon semiconductors. If noninteracting, such states correspond to half-occupied NBMOs which have energy levels in the middle of

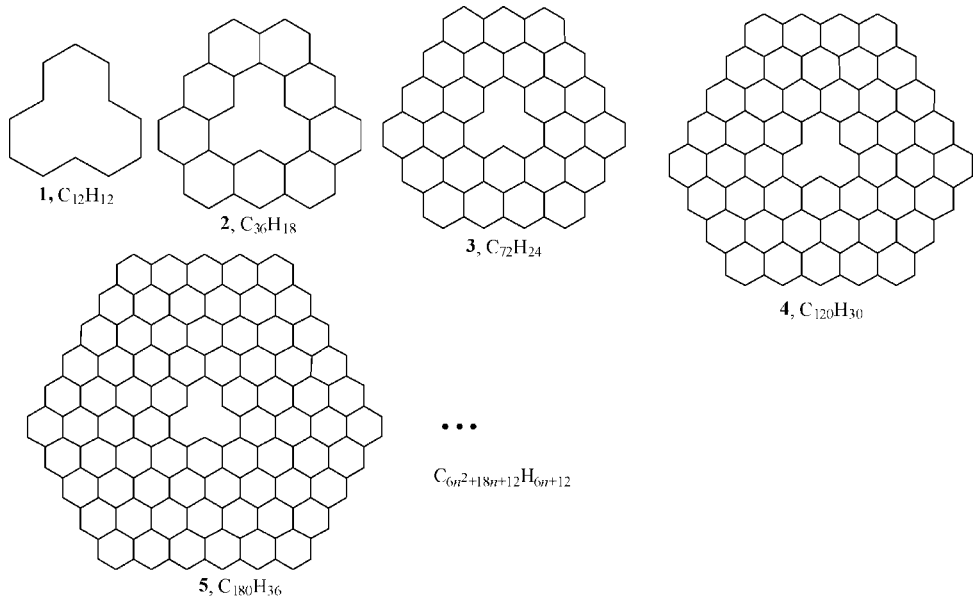

Figure 11. Polycircum[9]coronaphene hydrocarbon series. Note that **1**, **3**, **5**,... are doubly degenerate in the eigenvalues of zero, and according to Aihara,[39] **2** is "marginally antisuperaromatic".

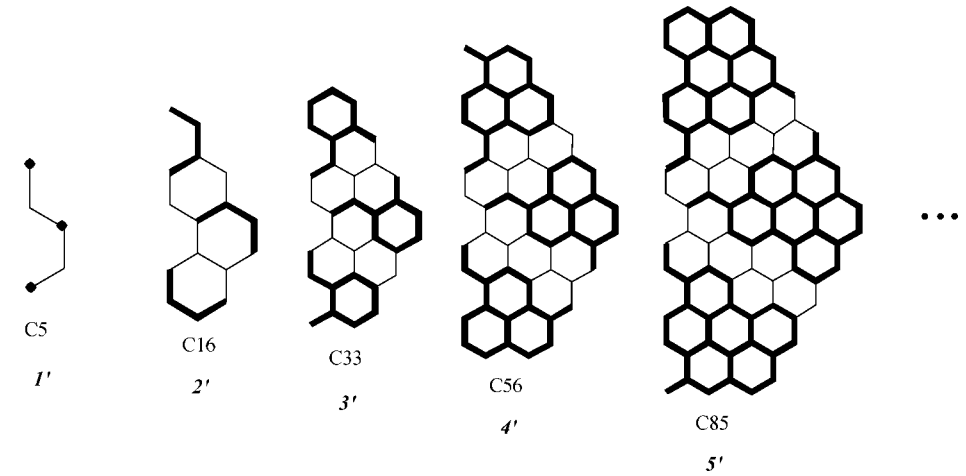

Figure 12. Right-hand mirror-plane fragments (McClelland subgraphs) belonging to the series in Figure 11. The odd-carbon systems being AHs must possess one zero eigenvalue. Using the zero-sum rule, one can easily derive the HMO coefficients to the antisymmetic NBMO. These McClelland subgraphs contain one set of doubly degenerate eigenvalues and the unique eigenvalues belonging to the embedding fragments (Hall subgraphs shown in bold).

the energy gap. These unstable polyradical systems undergo Jahn−Teller distortion, called surface reconstruction.[43] Alternatively, they may react with oxygen or engage in benzyne-like interactions, depending on the edge topology as discussed by Dietz and co-workers.[44]

Figure 9 shows three examples of interacting dangling sp^2 σ-orbitals within vacancy defects. The first example corresponds to the methyl antimolecule, where the three inner dangling bonds interact in analogy to the inner orbitals of the Walsh cyclopropane model, which is analogous to the HMO pπ-electronic solution to the cyclopropenyl radical; ionization of a single electron from this vacancy hole should result in it having aromatic character. The second example corresponds to the ethene antimolecule, where the inner dangling bonds interact in analogy to cyclobutadiene with two short bonds and two long ones reinforced by Jahn−Teller distortion, both of which negate possible antiaromatic character that would otherwise be conveyed to the vacancy. The third example corresponds to the benzene antimolecule, where the inner dangling bonds interact in analogy to benzene, resulting in a hole with aromatic character. This vacancy has both an 18 pπ aromatic perimeter and an sp^2 σ aromatic core of six electrons. In a magnetic field, one can visualize reinforcing concurrent-rotating ring diamagnetic currents in this vacancy.[45]

A hexaazakekulene ($C_{42}H_{18}N_6$) D_{6h} isomer shown in Figure 10 has six cavity nitrogens that need no inner hydrogen atom supplements and was the ultimate synthetic goal of a study by Ransohoff and Staab which was unsuccessful.[33] It should now be apparent that the 6 interacting nonbonding electron pairs in the cavity of this hexaazakekulene would be antiaromatic, thus explaining the lack of success in its synthesis. These electron delocalizations within the vacancy holes are similar to the electron delocalization at the periphery of the dication of hexaiodobenzene.[46]

Double and Triple Coronoids. Coronoid hydrocarbons with two holes are double coronoids and with three holes triple coronoids. These systems have been the subject of study starting with the first depiction of the smallest double coronoid by Dias[47] followed by a theoretical study by Hall.[6] The smallest triple coronoid was also first depicted by Dias.[47] These results initiated

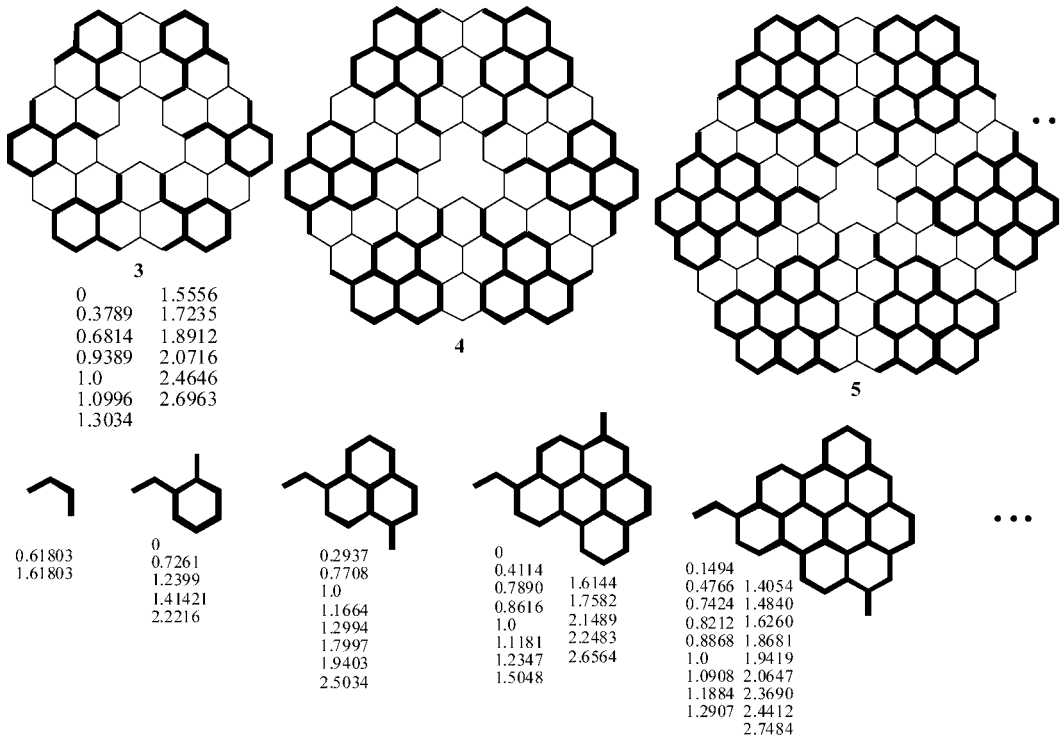

Figure 13. When smaller molecular graphs (bold) can be embedded in larger ones following Hall's rules, the eigenvalues of the smaller molecular graph (listed below each) can be found among the eigenvalues of the larger one. One set of doubly degenerate eigenvalues are listed for **3** below it.

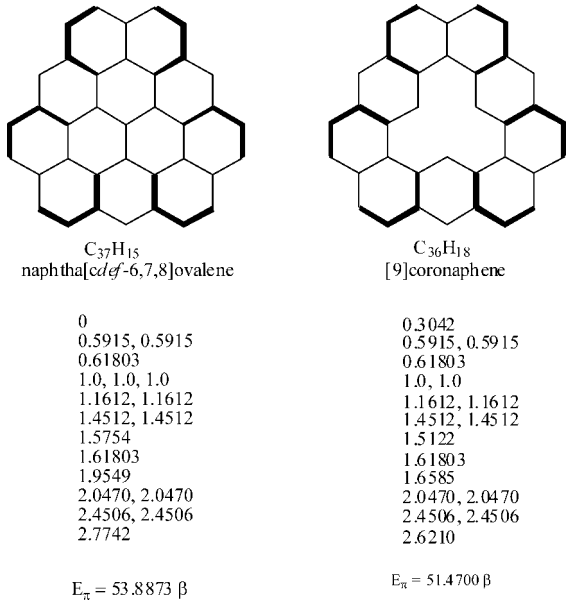

Figure 14. Eigenvalues of naphth[*cdef* −6,7,8]ovalene and [9]coronaphene. The 1,3-butadiene embedded fragments (Hall subgraphs) are shown in bold. Molecular graphs with greater than 2-fold symmetry will have 2/3 of their eigenvalues doubly degenerate.

further studies by Cyvin and co-workers and Trinajstić and co-workers.[48] We have an interest in double coronoids as models for the study of coalescence of graphitic vacancy hole defects. The energy change in a set of isomeric double coronoids as the holes move closer to each other and ultimately merge into a single hole is under current investigation.

Antiaromatic Macrocyclic Conjugation Contributions. Recently, Aihara showed that [9]coronaphene (Figure 1) is "marginally antisuperaromatic", which means that there is extra destabilization due to the macrocyclic conjugation contribution, although the entire π system is highly aromatic.[39] The presence of doubly degenerate NBMOs in a Kekluléan AH at the HMO computational level is a characteristic of antiaromatic molecules. Both cyclobutadiene (C_4H_4) and 1,3,5,7,9,11-cyclododecahexaene (**1**, $C_{12}H_{12}$) are well-known antiaromatic AHs with doubly degenerate zero eigenvalues. Herein we show that successive circumscription of antiaromatic **1** generates a series where every other member has a pair of degenerate NBMOs (two zero eigenvalues). This polycircum[9]coronaphene series is shown in Figure 11. The characteristic polynomial to **1**, **3**, **5**, **7**,... has zero tail coefficients. This must be true because their right-hand mirror-plane fragments (the McCelland subgraphs **1′**, **3′**, **5′**, **7′**,...)[30] shown in Figure 12 are OAHs (odd alternant hydrocarbons) and must have one zero eigenvalue, which by the pairing theorem mandates that **1**, **3**, **5**, **7**,... be degenerate in the eigenvalues of zero.[30,49−51] Figure 13 shows the embedding per Hall's rules,[30] which again demonstrates that the Kekluléan coronoids **3**, **5**, **7**,... must have two zero eigenvalues. Coronoids **3**, **5**, **7**,... represent the first examples of Kekuléan PAHs that are doubly degenerate in the eigenvalues of zero. Coronoids **3**, **5**, **7**,... having doubly degenerate zero eigenvalues and inner C12 and outer $4n$ ($n = 24j + 12$; $j = 1, 2, 3,...$) macrocyclic circuits might have somewhat more enhanced antiaromatic contributions, particularly for the first few members. Antikekulene is a $C_{36}H_{12}$ coronoid with an equal number of alternating benzene and cyclobutadiene rings and is overall strongly antiaromatic because of the dominance of the antiaromaticity of the cyclobutadiene rings and the macrocyclic inner C12 and outer C24 circuits.[39]

Optimal Vacancy Defects in Graphite. Figure 13 illustrates other pertinent points. Trends in the series of Hall subgraphs (the lower molecular graphs in Figure 13) should mirror the trends in the larger molecular graphs. Molecular graphs with greater than 2-fold symmetry contain preponderance (2/3 plus accidental degeneracy) of doubly degenerate eigenvalues, and

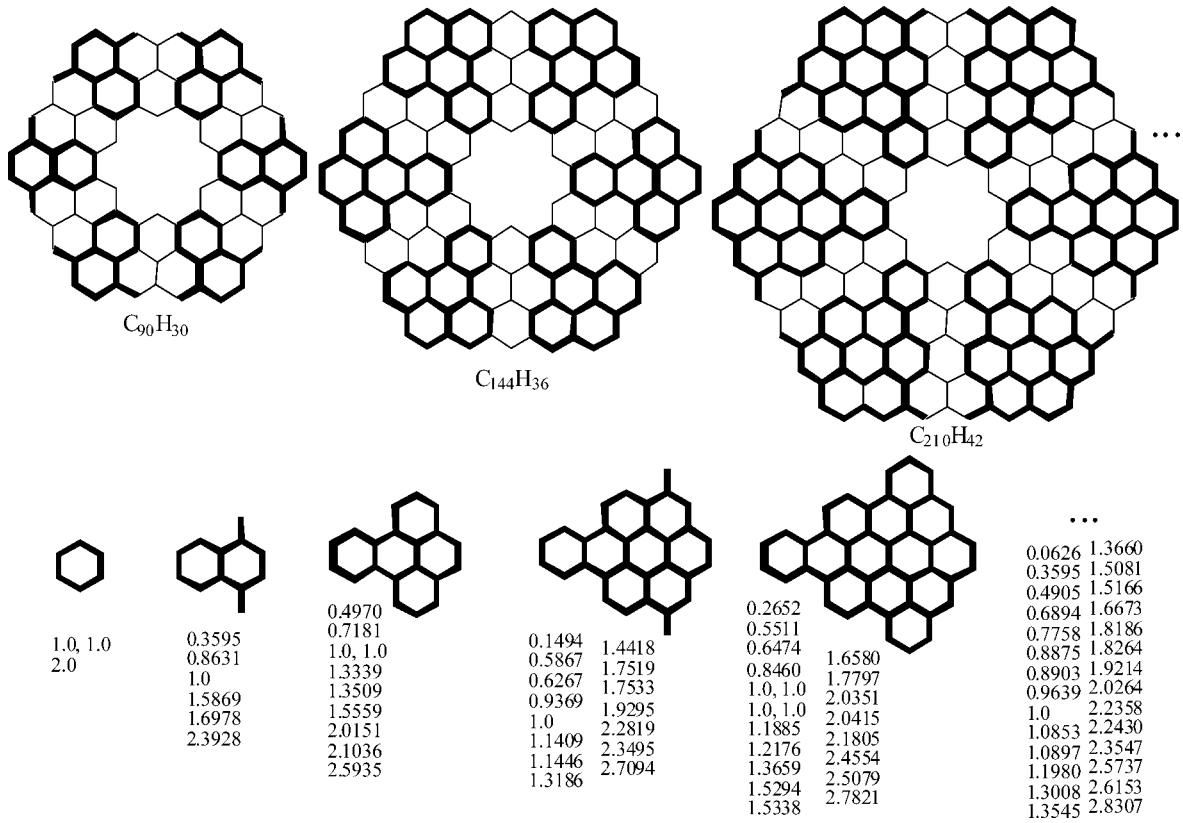

Figure 15. Polycircumkekulene series with their Hall subgraphs shown in bold and the corresponding eigenvalues listed below.

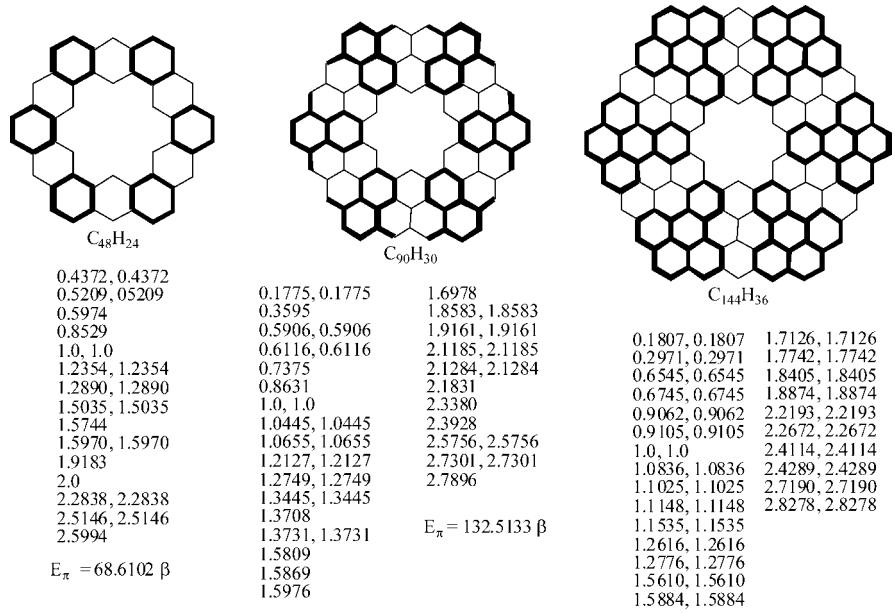

Figure 16. Eigenvalues for the $C_{48}H_{24}$, $C_{90}H_{30}$, and $C_{144}H_{36}$ members of the D_{6h} polycircumkekulene series ($C_{12n^2}+48n+36H_{6n+18}$); only the doubly degenerate eigenvalues are given for the latter.

the eigenvalues given for the Hall subgraphs shown are among the unique ones. Figure 14 illustrates this doubly degenerate principle with the $C_{37}H_{15}$ (circumphenalenyl monoradical) second-generation member of our constant D_{3h} 1-isomer series from Figure 2 and [9]coronaphene (**2**, $C_{36}H_{18}$) in Figure 1. [9]Coronaphene is generated by deletion of the central carbon vertex from circumphenalenyl monoradical. Recall that the latter is also derived from phenalenyl monoradical via our algorithm described in Figure 3. Thus, every corresponding pair from our constant D_{3h} 1-isomer series and the series in Figure 13 with 3-fold symmetry have the same Hall subgraphs and more than 2/3 of their eigenvalues in common as illustrated in Figure 14 for the monradical naphtha[*cdef*-6,7,8]ovalene (circumphenalenyl monoradical) and [9]coronaphene. The consequence of this is that the creation of a centrally located single-carbon atom vacancy defect in a 3-fold symmetrical graphite crystal layer (or the infinite graphite layer) should have a lower energy of activation than otherwise because there will be a minimum electronic reorganization associated with this process; more than 2/3 of the eigenvalues remain unchanged—the doubly degenerate ones and those due to embedding. From the HOMO of the Hall subgraphs, it is evident that the HOMO of the even-numbered

polycircum[9]coronaphenes in Figure 13 must approach zero as the members increase in size. Previously we demonstrated that if the ultimate excised internal structure is a nondisjoint diradical, then the strictly pericondensed parent structure also has to be a diradical.[52]

Polycircumkekulene Series. Successive circumscribing of kekulene leads to the polycircumkekulene series in Figure 15. The eigenvalues for the first two members plus only the doubly degenerate ones for the latter are given in Figure 16. Kekulene is one of eleven primitive $C_{48}H_{24}$ coronoids. All members of this series have D_{6h} symmetry, a doubly degenerate set of eigenvalues, and Hall subgraphs. Like the prior series, their McClelland subgraphs contain one set of doubly degenerate eigenvalues and the eigenvalues contained in their corresponding Hall subgraphs; these latter (unique) eigenvalues are given at the bottom of Figure 15. Their left-hand mirror-plane fragments (not given) contain the other set of doubly degenerate eigenvalues and the remaining unique eigenvalues.

There is a marked contrast between the polycircum[9]coronaphene series in Figure 11 and the polycircumkekulene series in Figure 15. The members belonging to the former series all have antiaromatic $4n$ annulene-like inner and outer circuits where the inner rim always comprises a 12 π conjugated pathway and the members belonging to the latter series all have aromatic $4n + 2$ inner and outer circuits where the inner rim always has an 18 π conjugated pathway. According to the dangling bond scenario (Figure 9), the single-atom vacancy in the former series should become aromatic upon ionization removal of a single electron and the antimolecule of the latter series should be aromatic.

Conclusion

A general algorithm and new isomer enumeration results of select primitive coronoid subclasses have been presented. When one compares the fibonacenic coronoids with their remaining primitive isomers, they turn out to have the highest K of all primitive coronoids just like the TRS benzenoids have the highest K compared to their remaining ordinary benzenoid isomers. Explanations for the failed syntheses of the $C_{36}H_{18}$ primitive coronoid ([9]coronaphene) and hexaazakekulene have been suggested, and TRS coronoids offer the most likely targets for future synthesis. A substantial amount of supportive eigenvalue data is presented. A series of coronoids with doubly degenerate eigenvalues of zero approaching graphite with a hole vacancy defect have been identified for the first time. The energy of activation for creation of a single carbon atom in graphite should be substantially more favorable than for other vacancy sizes. Both the polycircum[9]coronaphene (Figures 11 and 13) and polycircumkekulene (Figure 15) series appear to approach a zero band gap for their infinite members where the initial members of the first series have antiaromatic contributions and the latter do not. This work again demonstrates that our periodic benzenoid hydrocarbons (Table PAH6)[3,8,11,27] provide a unified framework for the study of select subclasses of benzenoids and related polyhex systems, and a comprehensive list of key lead references on the field of coronoid hydrocarbons can be found herein.

References and Notes

(1) Wu, J.; Pisula, W.; Müllen, K. *Chem. Rev.* **2007**, *107*, 718–747.

(2) (a) Dietz, F.; Tyutyukov, N.; Madjarova, G.; Müllen, K. *J. Phys. Chem. B* **2000**, *104*, 1746–1761. (b) Dietz, F.; Tyutyukov, N. *Chem. Phys. Lett.* **1999**, *246*, 255265;(c) Tyutyukov, N.; Madjarova, G.; Dietz, F.; Müllen, K. Energy spectra of giant polycyclic aromatic hydrocarbons. *J. Phys. Chem. B* **1998**, *102*, 10183–10189.

(3) Dias, J. R. *J. Phys. Chem. A* **2008**, *112*, 3260–3274.

(4) (a) Ebbesen, T. W. *Acc. Chem. Res.* **1998**, *31*, 558–566. (b) Balaban, A. T.; Klein, D. J.; Liu, X. *Carbon* **1994**, *32*, 357–359.

(5) Giordana, A.; Maranzana, A.; Ghigo, G.; Causa, M.; Tonachini, G. *J. Phys. Chem. A* **2008**, *112*, 973–982.

(6) (a) Hall, G. G. *Theor. Chim. Acta* **1988**, *73*, 425–435. (b) Dias, J. R. *J. Chem. Inf. Comput. Sci.* **1990**, *30*, 251–256.

(7) (a) Cyvin, S. J.; Brunvoll, J.; Cyvin, B. N. *Theory of Coronoid Hydrocarbons*; Lecture Notes in Chemistry; Springer-Verlag: Berlin, 1991. (b) Cyvin, S. J.; Brunvoll, J.; Chen, R. S.; Cyvin, B. N.; Zhang, F. J. *Theory of Coronoid Hydrocarbons II*; Lecture Notes in Chemistry, Vol. 62; Springer-Verlag: Berlin, 1994. (c) Balaban, A. T.; Brunvoll, J.; Cioslowski, J.; Cyvin, B. N.; Cyvin, S. J.; Gutman, I.; He, W. C.; He, W. J.; Knop, J. V.; Kovačević, M.; Müller, W. R.; Szymanski, K.; Tošić, R.; Trinajstić, N. *Z. Naturforsch.* **1987**, *42a*, 863–870.

(8) (a) Dias, J. R. *Chem. Phys. Lett.* **1991**, *176*, 559–562. (b) Dias, J. R. B. *J. Chem. Inf. Comput. Sci.* **1991**, *31*, 89–96. (c) Balaban, A. T.; Schmalz, T. G. *J. Chem. Inf. Model.* **2006**, *46*, 1563–1579. (d) Dias, J. R. *J. Chem. Inf. Model.* **2007**, *47*, 20–24.

(9) Staab, H. A.; Diederich, F. *Chem. Ber.* **1983**, *116*, 3487–3503.

(10) Funhoff, D. J. H.; Staab, H. A. *Angew. Chem., Int. Ed. Engl.* **1986**, *25*, 742–744.

(11) (a) Dias, J. R. *J. Chem. Inf. Comput. Sci.* **1990**, *30*, 251–256. (b) Dias, J. R. *J. Mol. Struct.: THEOCHEM* **1991**, *230*, 155–190.

(12) Keller, A.; Kovacs, R.; Homann, K.-H. *Phys. Chem. Chem. Phys.* **2000**, *2*, 1667–1675.

(13) Staab, H. A.; Sauer, M. *Liebigs Ann. Chem.* **1984**, 742–760.

(14) Randić, M. *Chem. Rev.* **2003**, *103*, 3449–3605.

(15) Brunvoll., J.; Cyvin, B. N.; Cyvin, S. J. *J. Chem. Inf. Comput. Sci.* **1987**, *27*, 14–21.

(16) Scott, L. T. *Pure Appl. Chem.* **1996**, *68*, 291–300.

(17) Dias, J. R. *J. Chem. Inf. Comput. Sci.* **1991**, *31*, 2–11.

(18) (a) Sattler, K. *Carbon* **1995**, *33*, 915–920. (b) Klein, D. J.; Balaban, A. T. *J. Chem. Inf. Model.* **2006**, *46*, 307–320.

(19) Yamamoto, K.; Harada, T.; Okamoto, Y.; Chikamatsu, H.; Nakazaki, M.; Kai, Y.; Nakao, T.; Tanaka, M.; Harada, S.; Kasai, N. *J. Am. Chem. Soc.* **1988**, *110*, 3578–3584.

(20) Yammamoto, K. *Pure Appl. Chem.* **1993**, *65*, 157–163.

(21) Lahti, P. M. *J. Org. Chem.* **1988**, *53*, 4590–4593.

(22) Dias, J. R. *J. Chem. Inf. Model.* **2005**, *45*, 562–571.

(23) (a) Brunvoll, J.; Cyvin, B. N.; Cyvin, S. J.; Gutman, I.; Tošić, R.; Kovačević, M. *J. Mol. Struct.: THEOCHEM* **1989**, *184*, 165–177.

(24) (a) Knop, J. V.; Müller, W. R.; Syzmanski, K.; Trinajstić, N. *Computer Generation of Certain Classes of Molecules*; SKTH/Kemija u industriji: Zagreb, Croatia, 1985. (b) Stojmenović, I.; Tošić, R.; Doroslavački, R. In *Generating and Counting Hexagonal Systems. Graph Theory*, Proceedings of the Sixth Yugoslav Seminar on Graph Theory, Dubrovnik, Croatia, 1985; Tosić, R., Aceta, D., Petrović, V., Eds.; University of Novi Sad: Novi Sad, Serbia, 1986; pp 189−197.

(25) Cyvin, S. J.; Brunvoll, J.; Cyvin, B. N.; Bergan, J. L.; Brendsdal, E. *Struct. Chem.* **1991**, *2*, 555–566.

(26) Balaban, A. T.; Randić, M. *J. Chem. Inf. Comput. Sci.* **2004**, *44*, 50–59.

(27) Dias, J. R. *J. Chem. Inf. Comput. Sci.* **2004**, *44*, 1210–1220.

(28) Cyvin, S. J.; Brunvoll, J.; Cyvin, B. N. *J. Chem. Inf. Comput. Sci.* **1990**, *30*, 210–222.

(29) (a) Müller, M.; Petersen, J.; Strohmaier, R.; Gunther, C.; Karl, N.; Müllen, K. *Angew. Chem., Int. Ed. Engl.* **1996**, *35*, 886–888. (b) Müller, M.; Kubel, C.; Müllen, K. *Chem.−Eur. J.* **1998**, *4*, 2099–2109. (c) Watson, M. D.; Fechtenkotter, A.; Müllen, K. *Chem. Rev.* **2001**, *101*, 1267–1300. (d) Dias, J. R. *J. Math. Chem.*, in press.

(30) Dias, J. R. *Molecular Orbital Calculations Using Chemical Graph Theory*; Springer-Verlag: Berlin, 1993; pp 15 and 29.

(31) Dötz, F.; Brand, J. D.; Ito, S.; Gherghet, L.; Müllen, K. *J. Am. Chem. Soc.* **2000**, *122*, 7707–7717.

(32) (a) Balaban, A. T. Chemical graphs. *Rev. Roum. Chim.* **1988**, *33*, 699–707. (b) Cyvin, B. N.; Cyvin, S. J.; Brunvoll, J. *Monatsh. Chem.* **1988**, *119*, 563–569. (c) Cyvin, S. J. *Monatsh. Chem.* **1989**, *120*, 243–252. (d) Cyvin, S. J.; Cyvin, B. N.; Brunvoll, J.; Hosoya, H.; Zhang, F.; Klein, D. J.; Chen, R.; Polansky, O. E. *Monatsh. Chem.* **1991**, *122*, 435–4444. (e) Cyvin, S. J.; Brunvoll, J.; Cyvin, B. N. *Struct. Chem.* **1990**, *1*, 429–436. (f) Cyvin, S. J. *Acta Chim. Hung.* **1990**, *127*, 849–864. (g) Klein, D. J.; Trinajstić, N. *J. Molec. Struct.: THEOCHEM* **1990**, *206*, 135–142.

(33) Ransohoff, J. E. B.; Staab, H. A. *Tetrahedron Lett.* **1985**, *26*, 6179–6182.

(34) Tatibouet, A.; Hancock, R.; Demeunynck, M.; Lhomme, J. *Angew. Chem., Int. Ed. Engl.* **1997**, *36*, 1190–1191.

(35) Dias, J. R.; Liu, B. *Monatsh. Chem.* **1990**, *121*, 13–30.

(36) Vogler, H. *J. Mol. Struct.: THEOCHEM* **1985**, *122*, 333–341.

(37) (a) Hosoya, H. *Top. Curr. Chem.* **1990**, *15*, 255–272. (b) Ohkami, N.; Hosoya, H. *Theor. Chim. Acta* **1983**, *64*, 153–170.

(38) Jiao, H.; von Rague Schleyer, P. *Angew. Chem., Int. Ed. Engl.* **1996**, *35*, 2383–2386.

(39) Aihara, J. *J. Phys. Chem. A* **2008**, *112*, 4382–4385.
(40) Cohen, N.; Benson, S. W. *Chem. Rev.* **1993**, *93*, 2419–2438.
(41) (a) Klein, D. J.; March, N. H. *Int. J. Quantum Chem.* **2001**, *85*, 327–344. (b) Ivanciuc, O.; Klein, D. J.; Bytautas, L. *Carbon* **2002**, *40*, 2063–2083. (c) Ivanciuc, O.; Bytautas, L.; Klein, D. J. *J. Chem. Phys.* **2002**, *116*, 4735–4748. (d) Klein, D. J.; Bytautas, L. *J. Phys. Chem. A* **1999**, *103*, 5196–5210.
(42) Randí; c, M.; Henderson, L. L.; Stout, R.; Trinajstić, N. *Int. J. Quantum. Chem., Quantum Chem. Symp.* **1988**, *22*, 127–141.
(43) Harrison, W. A. Electronic structure and properties of solids. *Surface and Defects*; W. H. Freeman & Co.: San Francisco, 1980; Chapter 10.
(44) Dietz, F.; Tyutyulkov, N.; Madjarova, G.; Mullen, K. *J. Phys. Chem. B* **2000**, *104*, 1746–1761.
(45) (a) Steiner, E.; Fowler, P. W.; Jenneskens, L. W.; Acocella, A. *Chem. Commun.* **2001**, 659–660. (b) Steiner, E.; Fowler, P. W.; Jenneskens, L. W. *Angew. Chem., Int. Ed.* **2001**, *40*, 362–365.
(46) Ciofini, I.; Lainé, P. P.; Adamo, C. *Chem. Phys. Lett.* **2007**, *435*, 171–175.
(47) Dias, J. R. *J. Chem. Inf. Comput. Sci.* **1984**, *24*, 124–135.
(48) (a) Cyvin, S. J.; Cyvin, B. N.; Brunvoll, J. *Chem. Phys. Lett.* **1989**, *156*, 595–599. (b) Knop, J. V.; Müller, W. R.; Szymanski, K.; Trinajstić, N. *J. Mol. Struct.: THEOCHEM* **1990**, *205*, 361–365. (c) Brunvoll, J.; Cyvin, S. J.; Cyvin, B. N.; Knop, J. V.; Müller, W. R.; Szymanski, K.; Trinajstić, N. *J. Mol. Struct.: THEOCHEM* **1990**, *207*, 131–139. (d) Cyvin, S. J.; Brunvoll, J.; Cyvin, B. N. *J. Chem. Inf. Comput. Sci.* **1989**, *29*, 236–244. (e) Cyvin, S. J.; Brunvoll, J.; Cyvin, B. N. *J. Chem. Inf. Comput. Sci.* **1990**, *30*, 210–222. (f) Cyvin, S. J.; Brunvoll, J. *Chem. Phys. Lett.* **1990**, *170*, 364–367. (g) Brunvoll, J.; Cyvin, B. N.; Cyvin, S. J. *Croat. Chem. Acta* **1990**, *63*, 585–601.
(49) McClelland, B. J. *J. Chem. Soc., Faraday Trans. 2* **1974**, *70*, 1453−1456; **1982**, *78*, 911−916; *Mol. Phys.* **1982**, *45*, 189−190.
(50) (a) Hall, G. G. *Inst. Math. Appl.* **1981**, *17*, 70–72. (b) Hall, G. G. *Trans. Faraday Soc.* **1957**, *53*, 573–581.
(51) Cash, G. G.; Dias, J. R. *J. Math. Chem.* **2001**, *30*, 429–444.
(52) Dias, J. R. *J. Chem. Inf. Comput. Sci.* **2003**, *43*, 1494–1501.

JP806987F